EUROPEAN TRANSACTIONS ON TELECOMMUNICATIONS
Eur. Trans. Telecomms. 2010; **21**:417–425
Published online 8 June 2010 in Wiley InterScience
(www.interscience.wiley.com) DOI: 10.1002/ett.1427

Comparison of different channel estimation approaches for Block-IFDMA†

A. Sohl* and A. Klein

Communications Engineering Lab, Technische Universität Darmstadt, Merckstr. 25, 64283 Darmstadt, Germany

SUMMARY

In this paper, channel estimation for Discrete Fourier Transform (DFT) precoded Orthogonal Frequency Division Multiple Access (OFDMA) with block-interleaved subcarrier allocation per user, which is denoted as Block-Interleaved Frequency Division Multiple Access (B-IFDMA), is considered. Recent investigations are presented for new pilot insertion methods which exhibit different impact on the Peak-to-Average Power Ratio (PAPR) of the transmit signal and offer different possibilities of positioning the pilots in frequency domain. Each of these pilot insertion methods is combined with a corresponding algorithm to estimate the Channel Variations in Frequency Domain (CVFD). The Channel Variations in Time Domain (CVTD) are estimated by an improved Decision Directed Channel Estimation (DDCE) with joint iterative Wiener filtering which reduces the error propagation by considering certain neighbouring symbols jointly in each iteration step. The DDCE is compared to a Wiener interpolation filter for the estimation of CVTD. The combinations of pilot insertion method, estimation algorithm for CVFD and CVTD are compared in terms of the PAPR and the Mean Square Error (MSE) performance. Thereby, the impact of different pilot positions in frequency domain and time domain is investigated. Copyright © 2010 John Wiley & Sons, Ltd.

1. INTRODUCTION

Within the ongoing research activities of future mobile radio systems, Discrete Fourier Transform Discrete Fourier Transform (DFT) precoded Orthogonal Frequency Division Multiple Access Orthogonal Frequency Division Multiple Access (OFDMA) is a candidate multiple access scheme for the non-adaptive uplink transmission. In this paper, the focus is on DFT precoded OFDMA in which the data of a specific user are transmitted on blocks of K_{F} adjacent subcarriers that are equidistantly distributed over the available bandwidth. This subcarrier allocation in connection with a DFT precoding leads to the so-called Block-Interleaved Frequency Division Multiple Access (B-IFDMA), as blocks of subcarriers assigned to different users are interleaved to each other [1]. B-IFDMA is a generalisation of the well-known Interleaved Frequency Division Multiple Access (IFDMA), where a block consists of a single subcarrier [2]. Due to the blockwise allocation, B-IFDMA is assumed to exhibit higher robustness against carrier frequency offsets than IFDMA and, at the same time, it maintains the advantage of high frequency diversity. In terms of channel estimation, another advantageous aspect of B-IFDMA compared to IFDMA is the support of interpolation in Frequency Domain (FD) within each block of K_{F} adjacent subcarriers. In Time Domain (TD), B-IFDMA can be combined with an additional user separation *via* a Time Division Multiple Access (TDMA) component. During one TDMA slot, each user is assigned to K successively transmitted B-IFDMA symbols. For each user, this opens up the possibility to enter a micro sleep mode

* Correspondence to: Anja Sohl, Communications Engineering Lab, Technische Universität Darmstadt, Merckstr. 25, Germany. E-mail: a.sohl@nt.tu-darmstadt.de
† A previous version of this paper was presented in the 7th International Workshop on Multi-Carrier System & Solutions (MC-SS 2009), Herrsching, Germany.

Received 19 March 2010
Accepted 30 March 2010

and to achieve considerable energy savings if K is small compared to the interval between consecutive TDMA slots [3].

In this paper, the B-IFDMA system with additional user separation *via* a TDMA component is investigated in terms of channel estimation issues. Our contributions include recent investigations on different pilot insertion methods for B-IFDMA. The first pilot insertion method keeps the orthogonality between pilots and data in FD and allows the variation of the pilot positions in FD. The drawback of this method is comprised in the increasing Peak-to-Average Power Ratio (PAPR) of the transmit signal. Therefore, in this paper, a new pilot insertion method is introduced which is promising in terms of a low PAPR but destroys the orthogonality between pilots and data. The Channel Variations in Frequency Domain (CVFD) are estimated according to different estimation algorithms for the respective pilot insertion method. These pilot insertion methods and their corresponding algorithms to estimate the CVFD can be combined with different algorithms for the estimation of the Channel Variations in Time Domain (CVTD). In this paper, a conventional Wiener interpolation filter for the estimation of CVTD is compared to a Decision Directed Channel Estimation (DDCE). The DDCE principle is well-known and has been presented for Orthogonal Frequency Division Multiplexing (OFDM), e.g. amongst others, in Reference [4] and for DFT precoded OFDM in Reference [5]. In this paper, DDCE with joint iterative Wiener filtering is considered which aims at minimising the error propagation with the help of an iterative Wiener filtering within each estimation step that is applied jointly to a certain number of neighbouring B-IFDMA symbols [6]. Our contributions include the investigation of the different combinations of pilot insertion methods and estimation algorithms for CVFD and CVTD in terms of their influence on the PAPR of the B-IFDMA transmit signal and the Mean Square Error (MSE) performance. Further on, the MSE performance is utilised to analyse the influence of pilot positioning in FD and TD on the overall estimation performance for B-IFDMA. Moreover, the DDCE and the Wiener interpolation filter are compared in terms of their respective benefits for the application to B-IFDMA.

The paper is organised as follows. In Section 2, a system model is presented for B-IFDMA. Section 3 introduces different pilot insertion methods and the respective estimation algorithms to estimate the CVFD. In Section 4, the estimation of the CVTD is addressed. Section 5 contains the investigations on PAPR and MSE. Section 6 concludes the investigations.

Table 1. Notations.

$(\cdot)^*$	Conjugate complex of a vector / matrix
$(\cdot)^{\mathrm{T}}$, $(\cdot)^{\mathrm{H}}$	Transpose, Hermitian of a vector / matrix
$\mathrm{diag}\{\mathbf{a}\}$	Diagonal matrix having the vector $\mathbf{a}$ as its main diagonal
$\lfloor a \rceil$	Nearest integer smaller than or equal to a
$\bar{\mathbf{a}}$	FD representation of the vector $\mathbf{a}$

2. SYSTEM MODEL

In this section, a system model for B-IFDMA is presented. In the following, all signals are represented by their discrete time equivalents in the complex baseband. Vectors and matrices are denoted by lower and upper case boldfaced letters, respectively. Further notations used throughout this work are given in Table 1.

Assuming a system with U users, the data symbols transmitted by a user with index u at symbol rate $1/T_{\mathrm{S}}$ are grouped into a vector $\mathbf{d}_k^{(u)} = [d_{k,0}^{(u)}, \ldots, d_{k,Q-1}^{(u)}]^{\mathrm{T}}$ with index k, $k = 0, \ldots, K-1$, denoting the index of the B-IFDMA symbol. The data symbols $d_{k,q}^{(u)}$, $q = 0, \ldots, Q-1$ can be taken from the alphabet of a modulation scheme like Phase Shift Keying (PSK) or Quadrature Amplitude Modulation (QAM), that is applied to coded or uncoded bits. The assignment of the data symbols $d_{k,q}^{(u)}$ to the user specific set of Q subcarriers can be described by a $Q \times Q$ DFT precoding matrix $\mathbf{F}_Q$, an $N \times Q$ mapping matrix $\mathbf{M}^{(u)}$ and an $N \times N$ IDFT matrix $\mathbf{F}_N^{\mathrm{H}}$, where N denotes the number of available subcarriers in the system [3]. The mapping matrix $\mathbf{M}^{(u)}$ has to describe the allocation of Q/K_{F} blocks each consisting of K_{F} adjacent subcarriers to the user with index u. The mapping matrix $\mathbf{M}^{(u)}$ is characterised by its elements $[\mathbf{M}^{(u)}]_{n,q}$, with $n = 0, \ldots, N-1$ and $q = 0, \ldots, Q-1$, that are given by

$$\left[\mathbf{M}^{(u)}\right]_{n,q} = \begin{cases} 1 \; n = \left\lfloor \frac{q}{K_{\mathrm{F}}} \right\rfloor K_{\mathrm{F}} \left(\frac{N}{Q} - 1 \right) + q + u K_{\mathrm{F}} \\ 0 \text{ else} \end{cases} \quad (1)$$

The resulting kth B-IFDMA symbol of user u consisting of N chips at chip rate $1/T_{\mathrm{C}} = U/T_{\mathrm{S}}$ is given by

$$\mathbf{x}_k^{(u)} = \mathbf{F}_N^{\mathrm{H}} \cdot \mathbf{M}^{(u)} \cdot \mathbf{F}_Q \cdot \mathbf{d}_k^{(u)} = \left[x_{k,0}^{(u)}, \ldots, x_{k,N-1}^{(u)} \right]^{\mathrm{T}} \quad (2)$$

In order to avoid intersymbol and inter-carrier interference, a Cyclic Prefix (CP) with N_{G} elements is inserted in-between successive B-IFDMA symbols. The resulting B-IFDMA signal is transmitted over a channel with

DOI: 10.1002/ett

impulse response $\mathbf{h}_k^{(u)}$ and $L_C \leq N_G$ non-zero coefficients $h_{k,l}^{(u)}, l = 0, \cdots, L_C - 1$, at chip rate. The channel is assumed to be time-invariant during the transmission of one B-IFDMA symbol. At the receiver, the CP is discarded and the $N \times 1$ vector $\mathbf{r}_k^{(u)} = [r_{k,0}^{(u)}, \ldots, r_{k,N-1}^{(u)}]^T$ containing the received B-IFDMA symbol is considered at the Q allocated subcarriers. The transmission over the multipath channel can be described by a flat fading channel for each allocated subcarrier in FD [7]. With the $Q \times 1$ vectors $\bar{\mathbf{c}}_k^{(u)} = [\bar{c}_{k,0}^{(u)}, \ldots, \bar{c}_{k,Q-1}^{(u)}]^T$, $\bar{\mathbf{d}}_k^{(u)} = [\bar{d}_{k,0}^{(u)}, \ldots, \bar{d}_{k,Q-1}^{(u)}]^T$ and $\bar{\mathbf{v}}_k^{(u)} = [\bar{v}_{k,0}^{(u)}, \ldots, \bar{v}_{k,Q-1}^{(u)}]^T$ which contain the Q complex channel transfer coefficients, the DFT elements of the transmitted data symbols and the Additive White Gaussian Noise (AWGN), respectively, corresponding to the Q subcarriers that are allocated to a user with index u in the B-IFDMA symbol with index k, the received values on the Q allocated subcarriers can be described by Equation [3].

$$\bar{\mathbf{y}}_k^{(u)} = \mathbf{M}^{(u)^H} \cdot \mathbf{F}_N \cdot \mathbf{r}_k^{(u)} = \mathrm{diag}\{\bar{\mathbf{c}}_k^{(u)}\} \cdot \bar{\mathbf{d}}_k^{(u)} + \bar{\mathbf{v}}_k^{(u)} \quad (3)$$

3. ESTIMATION OF CHANNEL VARIATIONS IN FREQUENCY DOMAIN

3.1. Introduction

In this section, the pilot assisted estimation of the CVFD is presented. For this purpose, pilot symbols are inserted within a single B-IFDMA symbol at the transmitter which are used to estimate the CVFD. The estimation of the CVFD refers to the estimation of the Q channel transfer factors of the allocated subcarriers whereas the channel transfer factors of the remaining subcarriers in the system are disregarded for channel estimation. It is assumed that interpolation in-between different blocks of K_F subcarriers is not feasible due to a distance larger than the coherence bandwidth of the channel between neighbouring blocks. In the following, two pilot insertion methods are introduced. For each of these two methods, the signal generation for pilot insertion and the algorithms for estimating the CVFD are explained.

3.2. Subcarrierwise pilot insertion

3.2.1. Signal generation. For subcarrierwise pilot insertion, a subset of Q_P subcarriers out of the total number Q of subcarriers allocated to a certain user in the B-IFDMA symbol with index $k = \kappa$ is utilised for pilot transmission. The remaining $Q_D = Q - Q_P$ subcarriers are exploited by transmitting data symbols within the κth B-IFDMA symbol.

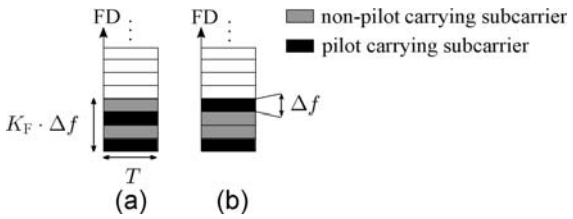

Figure 1. (a) Equidistant and (b) marginal pilot insertion in FD.

For $k = \kappa$, the vector $\boldsymbol{\rho}^{(u)} = [\rho_0^{(u)}, \cdots, \rho_{Q_P-1}^{(u)}]^T$ of Q_P pilot symbols with $E\{|\rho_q^{(u)}|^2\} = \sigma_P^2$ and the vector $\boldsymbol{\delta}_\kappa^{(u)} = [d_{\kappa,0}^{(u)}, \cdots, d_{\kappa,Q_D-1}^{(u)}]^T$ of data symbols with $E\{|d_{\kappa,q}^{(u)}|^2\} = \sigma_D^2$ are processed in parallel. The sequence $\boldsymbol{\rho}^{(u)}$ of pilot symbols is multiplied by a $Q_P \times Q_P$ DFT matrix $\mathbf{F}_{Q_P}$. The elements $\bar{\rho}_{q_P}^{(u)}, q_P = 0, \ldots, Q_P - 1$, of the resulting sequence $\bar{\boldsymbol{\rho}}^{(u)} = \mathbf{F}_{Q_P} \cdot \boldsymbol{\rho}^{(u)}$ of pilot symbols in FD are mapped onto a subset consisting of Q_P subcarriers out of the total number Q of subcarriers allocated to the user. In the following, two different methods of pilot insertion in FD are presented.

Equidistant pilot insertion Within each block of K_F subcarriers, every Ith subcarrier is used for pilot transmission. That means, $Q_P = \frac{Q}{I}$ subcarriers are used for pilot transmission where I is chosen such that $Q_P \in \mathbb{Z}$. The elements $\bar{\rho}_{q_P}^{(u)}$ are transmitted on subcarriers with indices

$$\eta(q_P) = \left\lfloor \frac{q_P \cdot I}{K_F} \right\rfloor K_F \left(\frac{N}{Q} - 1 \right) + q_P \cdot I + u \cdot K_F \quad (4)$$

which are denoted as pilot carrying subcarriers in the following. In Figure 1(a), the equidistant pilot insertion is sketched for $I = 2$.

Marginal pilot insertion Pilots are transmitted at the margins of each block of K_F subcarriers, i.e. $Q_P = \frac{2Q}{K_F}$ subcarriers are used for pilot transmission. The elements $\bar{\rho}_{q_P}^{(u)}$, $q_P = 0, \ldots, Q_P - 1$, are transmitted on subcarriers with indices

$$\eta(q_P) = \left\lfloor \frac{2q_P}{K_F} \right\rfloor \frac{K_F N}{Q} + (q_P \bmod 2) \cdot (K_F - 1) + u K_F \quad (5)$$

The marginal pilot insertion is sketched in Figure 1(b).

The allocation of the elements $\bar{\rho}_{q_P}^{(u)}, q_P = 0, \ldots, Q_P - 1$, to the pilot carrying subcarriers is performed by the application of the pilot mapping matrix $\mathbf{M}_P^{(u)}$ with the elements

DOI: 10.1002/ett

given by

$$\left[\mathbf{M}_{\mathrm{P}}^{(u)}\right]_{n,q_{\mathrm{P}}} = \begin{cases} 1 \; n = \eta(q_{\mathrm{P}}) \\ 0 \text{ else} \end{cases} \tag{6}$$

for $n = 0, \ldots, N-1$ and $q_{\mathrm{P}} = 0, \ldots, Q_{\mathrm{P}} - 1$. Simultaneously, the sequence $\boldsymbol{\delta}_{\kappa}^{(u)}$ of data symbols is multiplied by a $Q_{\mathrm{D}} \times Q_{\mathrm{D}}$ DFT matrix $\mathbf{F}_{Q_{\mathrm{D}}}$. The elements $\bar{d}_{\kappa,0}^{(u)}$, $q_{\mathrm{D}} = 0, \ldots, Q_{\mathrm{D}} - 1$, of the resulting sequence $\bar{\boldsymbol{\delta}}_{\kappa}^{(u)} = \mathbf{F}_{Q_{\mathrm{D}}} \cdot \boldsymbol{\delta}_{\kappa}^{(u)}$ of data symbols in FD are transmitted on the remaining Q_{D} non-pilot carrying subcarriers. The allocation of the elements $\bar{d}_{\kappa,0}^{(u)}$ to the non-pilot carrying subcarriers is realised by a data mapping matrix $\mathbf{M}_{\mathrm{D}}^{(u)}$. The superposition of the mapped pilot and mapped data symbols is multiplied by an $N \times N$ IDFT matrix $\mathbf{F}_N^{\mathrm{H}}$ and the B-IFDMA symbol $\mathbf{x}_{\kappa}^{(u)}$ containing pilot and data symbols is given by

$$\mathbf{x}_{\kappa}^{(u)} = \mathbf{F}_{\mathrm{N}}^{\mathrm{H}} \cdot \left(\mathbf{M}_{\mathrm{P}}^{(u)} \cdot \mathbf{F}_{Q_{\mathrm{P}}} \cdot \boldsymbol{\rho}^{(u)} + \mathbf{M}_{\mathrm{D}}^{(u)} \cdot \mathbf{F}_{Q_{\mathrm{D}}} \cdot \boldsymbol{\delta}_{\kappa}^{(u)} \right) \tag{7}$$

Finally, $\mathbf{x}_{\kappa}^{(u)}$ is expanded by a CP with N_{G} elements and is transmitted over the mobile radio channel.

3.2.2. Estimation algorithm. In this section, the channel estimation algorithm is explained for the subcarrierwise pilot insertion method.

At the receiver, the CP is discarded and the received B-IFDMA symbol $\mathbf{r}_{\kappa}^{(u)}$ is analysed at the pilot carrying subcarriers. Therefore, $\mathbf{r}_{\kappa}^{(u)}$ is multiplied by the $N \times N$ DFT matrix $\mathbf{F}_{\mathrm{N}}$ and the transpose $\mathbf{M}_{\mathrm{P}}^{(u)^{\mathrm{T}}}$ of the pilot mapping matrix. Then, an estimate for the channel transfer factors of the pilot carrying subcarriers in the B-IFDMA symbol with index κ is determined by a Least Square (LS) estimation and given by

$$\left[\hat{\bar{c}}_{\kappa,0}^{(u)}, \ldots, \hat{\bar{c}}_{\kappa,Q_{\mathrm{P}}-1}^{(u)}\right]^{\mathrm{T}} = \mathrm{diag}\left\{\bar{\boldsymbol{\rho}}^{(u)}\right\}^{-1} \cdot \mathbf{M}_{\mathrm{P}}^{(u)^{\mathrm{T}}} \cdot \mathbf{F}_N \cdot \mathbf{r}_{\kappa}^{(u)} \tag{8}$$

[8]. The LS estimates $\hat{\bar{c}}_{\kappa,q_{\mathrm{P}}}^{(u)}$, $q_{\mathrm{P}} = 0, \ldots, Q_{\mathrm{P}} - 1$, which correspond to the channel transfer factors of the pilot carrying subcarriers are exploited to get estimates $\hat{\bar{c}}_{\kappa,q_{\mathrm{D}}}^{(u)}$, $q_{\mathrm{D}} = 0, \ldots, Q_{\mathrm{D}} - 1$ for the channel transfer factors of the remaining, non-pilot carrying subcarriers.

For this purpose, two different interpolation methods are proposed in the following.

Wiener interpolation filter The Wiener interpolation filter is a Finite Impulse Response (FIR) filter with $\frac{Q_{\mathrm{P}} K_{\mathrm{F}}}{Q}$ filter coefficients that is applied to the LS estimates $\hat{\bar{c}}_{\kappa,q_{\mathrm{P}}}^{(u)}$ within each block of K_{F} subcarriers. The filter coefficients are derived such that the MSE between the estimated channel transfer factors and the true channel transfer factor becomes minimum [9, 10].

Finally, the LS estimates of the pilot carrying subcarriers and the Wiener filter estimates of the non-pilot carrying subcarriers are combined in the vector $\hat{\bar{\mathbf{c}}}_{\kappa}^{(u)}$.

Repetition For the case, that there is only one pilot carrying subcarrier per block of K_{F} subcarriers, i.e. $Q_{\mathrm{P}} = \frac{Q}{K_{\mathrm{F}}}$, the application of an interpolation filter is not feasible. Then, the LS-estimate of the nearest pilot carrying subcarrier is used for equalisation of the non-pilot carrying subcarriers within the same block of K_{F} subcarriers. Thus, the vector $\hat{\bar{\mathbf{c}}}_{\kappa}^{(u)}$ containing the channel estimates for each allocated subcarrier within the B-IFDMA symbol with index κ is given by

$$\hat{\bar{\mathbf{c}}}_{\kappa}^{(u)} = [\underbrace{\hat{\bar{c}}_{\kappa,0}^{(u)}, \hat{\bar{c}}_{\kappa,0}^{(u)}, \ldots}_{K_{\mathrm{F}}\text{-times}}, \ldots, \underbrace{\hat{\bar{c}}_{\kappa,Q_{\mathrm{P}}-1}^{(u)}, \hat{\bar{c}}_{\kappa,Q_{\mathrm{P}}-1}^{(u)}, \ldots}_{K_{\mathrm{F}}\text{-times}}]. \tag{9}$$

3.3. Chipwise pilot insertion

3.3.1. Signal generation. For chipwise pilot insertion, the transmit vector of the B-IFDMA symbol with index $k = \kappa$ contains Q_{P} pilot symbols and $Q_{\mathrm{D}} = Q - Q_{\mathrm{P}}$ data symbols.

For $k = \kappa$, the $Q \times 1$ vector $\boldsymbol{\rho}^{(u)} = [0, \ldots, 0, \rho_0^{(u)}, \cdots, \rho_{Q_{\mathrm{P}}-1}^{(u)}]^{\mathrm{T}}$ of Q_{P} pilot symbols with $\mathrm{E}\{|\rho_q^{(u)}|^2\} = \sigma_{\mathrm{P}}^2$ and the $Q \times 1$ vector $\boldsymbol{\delta}_{\kappa}^{(u)} = [d_{\kappa,0}^{(u)}, \cdots, d_{\kappa,Q_{\mathrm{D}}-1}^{(u)}, 0, \ldots, 0]^{\mathrm{T}}$ of data symbols with $\mathrm{E}\{|d_{\kappa,q}^{(u)}|^2\} = \sigma_{\mathrm{D}}^2$ are processed in parallel.

The superposition $\boldsymbol{\rho}^{(u)} + \boldsymbol{\delta}_{\kappa}^{(u)}$ of both vectors is multiplied by the $Q \times Q$ DFT matrix $\mathbf{F}_{\mathrm{Q}}$. The elements of the resulting vector are mapped onto the Q block-interleaved subcarriers in FD and transformed in TD *via* the $N \times N$ IDFT matrix $\mathbf{F}_N^{\mathrm{H}}$.

Thus, the sequence $\mathbf{x}_{\kappa}^{(u)}$ containing multiplexed pilot and data symbols is calculated by

$$\mathbf{x}_{\kappa}^{(u)} = \mathbf{F}_N^{\mathrm{H}} \cdot \mathbf{M}^{(u)} \cdot \mathbf{F}_Q \cdot \left(\boldsymbol{\rho}^{(u)} + \boldsymbol{\delta}_{\kappa}^{(u)} \right) \tag{10}$$

That means, on each allocated subcarrier, a superposition of pilot and data symbols in FD is transmitted. Due to the chipwise pilot insertion, pilot and data symbols are not orthogonal in FD.

DOI: 10.1002/ett

Finally, $\mathbf{x}_\kappa^{(u)}$ is expanded by a CP with N_G elements and transmitted over the mobile radio channel.

3.3.2. Estimation algorithm. In this section, the channel estimation algorithm is explained for the chipwise pilot insertion method.

For that purpose, the received symbol $\mathbf{r}_\kappa^{(u)}$ with index κ is considered after removal of the CP. $\mathbf{r}_\kappa^{(u)}$ is transformed into FD by multiplication with the $N \times N$ DFT matrix $\mathbf{F}_N$ and multiplied by the transpose $\mathbf{M}^{(u)^\mathrm{T}}$ of the mapping matrix which leads to the vector $\bar{\mathbf{y}}_\kappa^{(u)}$ in FD that is given by

$$\begin{aligned}\bar{\mathbf{y}}_\kappa^{(u)} &= \mathbf{M}^{(u)^\mathrm{T}} \cdot \mathbf{F}_N \cdot \mathbf{r}_\kappa^{(u)} \\ &= \mathrm{diag}\{\bar{\mathbf{c}}_\kappa^{(u)}\} \cdot \mathbf{F}_Q \cdot \left(\boldsymbol{\rho}^{(u)} + \boldsymbol{\delta}_\kappa^{(u)}\right) + \bar{\mathbf{v}}_\kappa^{(u)} \end{aligned} \quad (11)$$

$$\begin{aligned}[\bar{\mathbf{y}}_\kappa^{(u)}]_\mathrm{e} &= \mathrm{diag}\left\{[\bar{\mathbf{c}}_\kappa^{(u)}]_\mathrm{e}\right\} \cdot [\mathbf{F}_Q]_{\mathrm{e},:} \cdot \left(\boldsymbol{\rho}^{(u)} + \boldsymbol{\delta}_\kappa^{(u)}\right) + [\bar{\mathbf{v}}_\kappa^{(u)}]_\mathrm{e} \\ &= \mathrm{diag}\left\{[\bar{\mathbf{c}}_\kappa^{(u)}]_\mathrm{e}\right\} \cdot \left([\mathbf{F}_Q]_{\mathrm{e},Q_\mathrm{D}+1:Q} \cdot [\rho_0^{(u)}, \cdots, \rho_{Q_\mathrm{P}-1}^{(u)}]^\mathrm{T} + [\mathbf{F}_Q]_{\mathrm{e},1:Q_\mathrm{D}} \cdot [d_{\kappa,0}^{(u)}, \cdots, d_{\kappa,Q_\mathrm{D}-1}^{(u)}]^\mathrm{T}\right) + [\bar{\mathbf{v}}_\kappa^{(u)}]_\mathrm{e} \end{aligned} \quad (12)$$

$$\begin{aligned}[\bar{\mathbf{y}}_\kappa^{(u)}]_\mathrm{o} &= \mathrm{diag}\left\{[\bar{\mathbf{c}}_\kappa^{(u)}]_\mathrm{o}\right\} \cdot [\mathbf{F}_Q]_{\mathrm{o},:} \cdot \left(\boldsymbol{\rho}^{(u)} + \boldsymbol{\delta}_\kappa^{(u)}\right) + [\bar{\mathbf{v}}_\kappa^{(u)}]_\mathrm{o} \\ &= \mathrm{diag}\left\{[\bar{\mathbf{c}}_\kappa^{(u)}]_\mathrm{o}\right\} \cdot \left([\mathbf{F}_Q]_{\mathrm{o},Q_\mathrm{D}+1:Q} \cdot [\rho_0^{(u)}, \cdots, \rho_{Q_\mathrm{P}-1}^{(u)}]^\mathrm{T} + [\mathbf{F}_Q]_{\mathrm{o},1:Q_\mathrm{D}} \cdot [d_{\kappa,0}^{(u)}, \cdots, d_{\kappa,Q_\mathrm{D}-1}^{(u)}]^\mathrm{T}\right) + [\bar{\mathbf{v}}_\kappa^{(u)}]_\mathrm{o} \end{aligned} \quad (13)$$

$$\mathrm{diag}\left\{[\hat{\bar{\mathbf{c}}}_\kappa^{(u)}]_\mathrm{e}\right\} = \mathrm{diag}\left\{\left(\left([\mathbf{F}_Q]_{\mathrm{e},1:Q_D}\right)^\mathrm{H} \cdot \mathrm{diag}\{[\bar{\mathbf{y}}_\kappa^{(u)}]_\mathrm{e}\} - \left([\mathbf{F}_Q]_{o,1:Q_\mathrm{D}}\right)^\mathrm{H} \cdot \mathrm{diag}\{[\bar{\mathbf{y}}_\kappa^{(u)}]_\mathrm{o}\}\right)^{-1} \cdot \left[\rho_0^{(u)}, \ldots, \rho_{Q_\mathrm{P}-1}^{(u)}\right]^\mathrm{T}\right\}^{-1} \quad (14)$$

Let $[\mathbf{a}]_e$ denote a vector containing the elements with even indices of a vector $\mathbf{a}$, i.e. $[\mathbf{a}]_e = [\mathbf{a}]_{0:2:\mathrm{end}-2}$, and let $[\mathbf{a}]_\mathrm{o}$ denote a vector containing the elements with odd indices of a vector $\mathbf{a}$, i.e. $[\mathbf{a}]_\mathrm{o} = [\mathbf{a}]_{1:2:\mathrm{end}-1}$.

Then, the vector $\bar{\mathbf{y}}_\kappa^{(u)}$ can be separated into a vector $[\bar{\mathbf{y}}_\kappa^{(u)}]_\mathrm{e}$ containing the elements corresponding to the subcarriers with even indices and into a vector $[\bar{\mathbf{y}}_\kappa^{(u)}]_\mathrm{o}$ containing the elements corresponding to the subcarriers with odd indices, which are given in Equation (12) and (13), respectively. It can be seen, that both vectors are dependent on the same unknown data vector $[d_{\kappa,0}^{(u)}, \ldots, d_{\kappa,Q_\mathrm{D}-1}^{(u)}]^\mathrm{T}$ and the matrices containing the unknown channel transfer factors. Thus, Equation (12) and (13) can be combined in one equation where the data vector $[d_{\kappa,0}^{(u)}, \ldots, d_{\kappa,Q_\mathrm{D}-1}^{(u)}]^\mathrm{T}$ is eliminated. For the case that at least $K_\mathrm{F} = 2$ subcarriers per block are available and under the assumption that there is only slight variation between channel transfer factors corresponding to neighbouring subcarriers, i.e. $[\bar{\mathbf{c}}_\kappa^{(u)}]_\mathrm{e} \approx [\bar{\mathbf{c}}_\kappa^{(u)}]_\mathrm{o}$, an estimate $[\hat{\bar{\mathbf{c}}}_\kappa^{(u)}]_\mathrm{e}$ can be found by solving Equation (12) and (13) for $[\bar{\mathbf{c}}_\kappa^{(u)}]_\mathrm{e}$. The solution is shown in Equation (14) for the case of negligible AWGN.

4. ESTIMATION OF CHANNEL VARIATIONS IN TIME DOMAIN

4.1. Introduction

In this section, the pilot insertion for the estimation of the CVTD is explained. In Section 3, the subcarrierwise and chipwise pilot insertion have been introduced considering a single B-IFDMA symbol. The presented methods can be used to insert pilot symbols within P B-IFDMA symbols with indices $k = \kappa_1, \ldots, \kappa_\mathrm{P}$, in general. In the following, the B-IFDMA symbols with indices $k = \kappa_1, \ldots, \kappa_\mathrm{P}$ are referred to as pilot carrying B-IFDMA symbols, whereas the B-IFDMA symbols with indices $k \neq \kappa_1, \ldots, \kappa_\mathrm{P}$ are referred to as non-pilot carrying B-IFDMA symbols. It is assumed that interpolation between neighbouring TDMA slots of a certain user is not feasible due to a time interval between consecutive TDMA slots that is much larger than the coherence time of the channel. Therefore, in the following, a single TDMA slot consisting of K successively transmitted B-IFDMA symbols is considered. Further on, the following derivations refer to the signal of a single user with index u and, thus, the user index is omitted for simplicity reasons.

DOI: 10.1002/ett

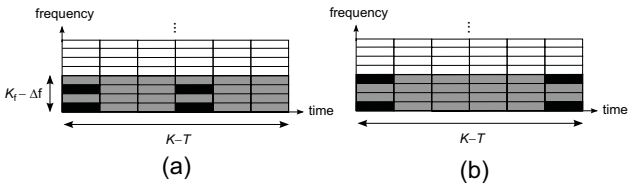

Figure 2. Pilot allocation for subcarrierwise equidistant pilot insertion in FD and (a) equidistant, (b) marginal pilot insertion with $P = 2$ in TD.

4.2. Wiener interpolation filter

The CVTD are estimated by a Wiener interpolation filter if $P \geq 2$ B-IFDMA symbols are utilised for pilot transmission. In analogy to Section 3.2, the pilot carrying B-IFDMA symbols can be allocated equidistantly within the K successively transmitted B-IFDMA symbols, *cf*. Figure 2(a), or at the margins of the K B-IFDMA symbols,*cf*. Figure 2(b).

For the pilot carrying B-IFDMA symbols with indices $k = \kappa_1, \ldots, \kappa_\mathrm{P}$, the vectors $\hat{\tilde{\mathbf{c}}}_{\kappa_1}, \ldots, \hat{\tilde{\mathbf{c}}}_{\kappa_\mathrm{P}}$ are available which contain the channel transfer factors that are estimated according to the subcarrierwise or chipwise pilot insertion, respectively. The vectors of channel transfer factors for the non-pilot carrying B-IFDMA symbols are derived by the application of a Wiener interpolation filter to $\hat{\tilde{\mathbf{c}}}_{\kappa_1}, \ldots, \hat{\tilde{\mathbf{c}}}_{\kappa_\mathrm{P}}$ according to Reference [10].

4.3. Decision directed estimation

In this section, the estimation of the CVTD is explained for DDCE with joint iterative Wiener filtering.

For the application of the proposed DDCE with joint iterative Wiener filtering only one pilot carrying B-IFDMA symbol is required, i.e. $P = 1$, and, thus, the DDCE is feasible where the application of Wiener interpolation filtering fails. In Table 2, the basic method of the DDCE with joint iterative Wiener filtering is outlined. It is applied after the channel transfer factors have been determined for each subcarrier, e.g. of the first symbol, *via* subcarrierwise pilot insertion with repetition or Wiener interpolation or chipwise pilot insertion. For B-IFDMA, the DDCE principle described in Reference [4] leads to a high noise amplification with increasing number K of B-IFDMA symbols. Therefore, we propose an algorithm where a Wiener filter is applied to the decision directed estimates and the filtered estimates are used iteratively for DDCE again. The innovation compared to the algorithm presented in Reference [6] comprises the joint iterative filtering of S decision directed channel estimates related to S neighbouring B-IFDMA symbols. In Table 2, the upper index denotes the iteration index and the Wiener filter coefficients $b_{-S+1}, \ldots, b_{S-1}$ are calculated according to Reference [10].

Table 2. DDCE with iterative Wiener filtering.

1. Initialisation

Equalisation with $\hat{\tilde{\mathbf{c}}}_0$

Estimation of transmitted symbols

$\rightarrow \hat{\tilde{\mathbf{d}}}_1^{(0)}, \cdots, \hat{\tilde{\mathbf{d}}}_S^{(0)}$

For $k = 1, \ldots, K-1$

2. Decision Directed Channel Estimation

$$\hat{\tilde{\mathbf{c}}}_k^{(k)} = \frac{\tilde{\mathbf{y}}_k}{\hat{\tilde{\mathbf{d}}}_k^{(k-1)}}, \cdots, \hat{\tilde{\mathbf{c}}}_{e_1}^{(k)} = \frac{\tilde{\mathbf{y}}_{e_1}}{\hat{\tilde{\mathbf{d}}}_{e_1}^{(k-1)}}$$

$$e_1 = \begin{cases} S & \text{for } k \leq S/2 \\ K-1 & \text{for } k > K - S/2 - 1 \\ k + S/2 - 1 & \text{else} \end{cases}$$

3. Wiener Filtering with S filter coefficients

$$\tilde{\tilde{\mathbf{c}}}_k = \sum_{s=e_2}^{0} b_s \cdot \hat{\tilde{\mathbf{c}}}_{k-s}^{(k)} + \sum_{s=1}^{e_3} b_s \cdot \tilde{\tilde{\mathbf{c}}}_{k-s}$$

$$e_2 = \begin{cases} k - S \\ k + 1 - K \\ -S/2 + 1 \end{cases} \quad e_3 = \begin{cases} k - 1 & , k \leq S/2 \\ S - K + k & , k > K - S/2 - 1 \\ S/2 & \text{else} \end{cases}$$

4. Equalisation with $\tilde{\tilde{\mathbf{c}}}_k$

Estimation of transmitted symbols

$\rightarrow \hat{\tilde{\mathbf{d}}}_{k+1}^{(k)}, \cdots, \hat{\tilde{\mathbf{d}}}_{e_1}^{(k)}$

end

5. PERFORMANCE ANALYSIS

5.1. Analysis assumptions

In this Section 5, the channel estimation approaches presented in Section 3 and Section 4 are analysed in terms of their influence on the PAPR of the transmit signal and their MSE performance. The results are obtained by computer simulations and are valid for the parameters summarised in Table 3.

Table 3. System parameters.

Carrier frequency	$f_0 = 3.7\,\mathrm{GHz}$
Bandwidth	$B = 40\,\mathrm{MHz}$
No. of subcarriers	$N = 1024$
Modulation	QPSK
Coding	Convolutional
Code rate,constraint length	1/2, 6
Decoder	MaxLogMAP [11]
Equalizer	Linear MMSE in FD [12]
Interleaving, depth	Random, 0.5 ms
Guard interval duration	$T_\mathrm{G} = 3.2\,\mu\mathrm{s}$
No. of B-IFDMA symbols	$K = 10$
Channel model	Typical Urban (COST 207) [13]
Coherence bandwidth	$B_\mathrm{coh} = 8\Delta f$
Pilot symbols	CAZAC sequence [14]

DOI: 10.1002/ett

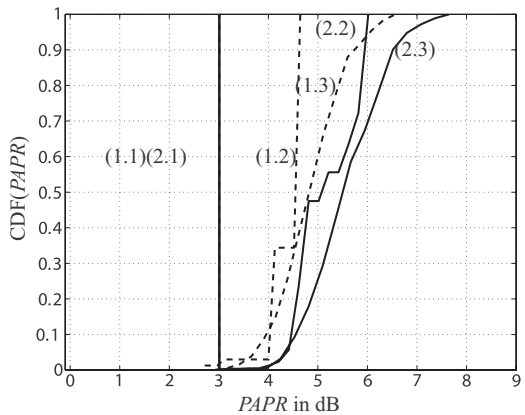

Figure 3. Cumulative Distribution Function (CDF) of the PAPR in case of (a) chipwise and (b) subcarrierwise pilot insertion with interpolation depth $I = 2$ for $Q = 32$ and (1.1)(2.1) $K_F = 2$, (1.2)(2.2) $K_F = 4$ and (1.3)(2.3) $K_F = 8$.

5.2. Peak-to-average power ratio

The PAPR per pilot carrying B-IFDMA symbol represents the ratio between the peak power and the average power within one pilot carrying B-IFDMA symbol and is defined for $n = -N_G, \ldots, N + N_G - 1$ as

$$PAPR = \max_n \left\{ \frac{|x_{\kappa,n}^{(u)}|^2}{E\{|x_{\kappa,n}^{(u)}|^2\}} \right\} \tag{15}$$

[15]. In Figure 3, the CDF of the PAPR per pilot carrying B-IFDMA symbol is presented in dependency of the PAPR in dB. The CDF describes the probability that the PAPR takes a value less than or equal to a certain realisation of the PAPR which is denoted by *PAPR*. Figure 3 shows the CDF of the PAPR in case of subcarrierwise and chipwise pilot insertion with $I = 2$ and $Q = 32$ allocated subcarriers per user. For the block size, the values $K_F = 2, 4, 8$ are investigated.

It can be seen that for $K_F = 2$, the PAPR is identical for subcarrierwise and for chipwise pilot insertion. For subcarrierwise pilot insertion, the transmit signal consists of the summation of two signals each with $K_F = 1$ subcarrier per block, i.e. the superposition of two IFDMA signals is transmitted. From this it can be deduced that the summation of two IFDMA signals exhibits the same PAPR as a B-IFDMA signal with $K_F = 2$ subcarriers per block.

If the blocksize is increased, the chipwise pilot insertion exhibits a maximum PAPR that is considerably lower than the maximum PAPR for subcarrierwise pilot insertion. That means, the chipwise pilot insertion is beneficial for blocksizes $K_F > 2$.

5.3. Mean square error

In this section, the performance of the estimation algorithms introduced in Section 3 and in Section 4 are investigated in terms of their MSE performance. The MSE is defined as

$$MSE = \frac{1}{Q \cdot K} \sum_{k=0}^{K-1} \|\hat{\tilde{\mathbf{c}}}_k^{(u)} - \tilde{\mathbf{c}}_k^{(u)}\|_2^2 \tag{16}$$

In Figure 4(a)–(c), the MSE is presented in dependency of the Signal-to-Noise Ratio (SNR) which is given as a logarithmic value of the ratio between the energy E_B that is spent per useful data bit and the noise power N_0. The calculation of the SNR takes into account the overhead due to channel coding and insertion of CP. Further on, the SNR degradation due to pilot symbol insertion is included in the SNR [16]. The presented curves are obtained from Monte-Carlo simulations whose results are averaged over 1000 simulation runs. In FD, every second subcarrier is used for pilot transmission ($Q_P = Q/2$). In TD, $P = 2$ pilot carrying B-IFDMA symbols are utilised for Wiener interpolation filtering and $P = 1$ pilot carrying B-IFDMA symbol is utilised for DDCE. Table 4 gives an overview of the presented

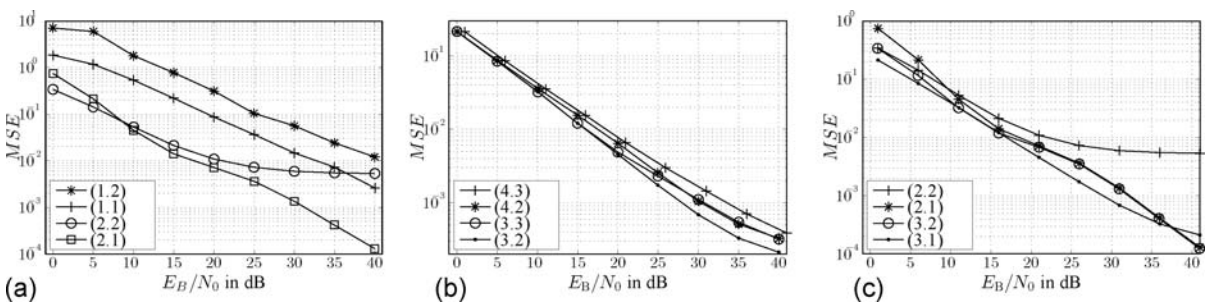

Figure 4. Comparison of (a) chipwise pilot insertion and subcarrierwise pilot insertion with repetition for the estimation of CVFD, (b) different pilot positions in FD and TD, (c) DDCE and Wiener interpolation filtering for the estimation of CVTD.

DOI: 10.1002/ett

Table 4. MSE result overview.

Time domain		Frequency domain			
				Subcarrier + Wiener	
		Chipwise	Subcarrier + Repetition	Marginal	Equidistant
	DDCE	(1.1) in Figure 4(a)	(2.1) in Figure 4(a), Figure 4(c)	(3.1) in Figure 4(c)	-
	marginal	(1.2) in Figure 4(a)	(2.2) in Figure 4(a), Figure 4(c)	(3.2) in Figure 4(b), Figure 4(c)	(4.2) in Figure 4(b)
Wiener	equidistant	-	-	(3.3) in Figure 4(b)	(4.3) in Figure 4(b)

results and shows the combinations of estimation algorithms for CVFD and CVTD. The presented results are valid for $Q = 16$ allocated subcarriers and a velocity of $v = 40$ km/h.

In Figure 4(a) the number of subcarriers per block is $K_F = 2$. The chipwise pilot insertion with its corresponding channel estimation algorithm is compared to the subcarrierwise pilot insertion with repetition. Therefore, both algorithms for the estimation of CVFD are combined with DDCE and Wiener interpolation filtering for the estimation of CVTD, respectively. It can be seen, that the performance of chipwise pilot insertion is very poor. The reason for that can be found in the double inversion in Equation (14). If the matrices that have to be inverted are ill-conditioned, the solution of the system of equations loses precision. Nevertheless, it can be stated that the application of DDCE for the estimation of CVTD improves the performance of chipwise pilot insertion significantly compared to the combination with Wiener filtering.

Figure 4(b) presents the influence of the pilot positions in FD and TD for the case that Wiener filtering is applied for the estimation of CVFD and CVTD. The blocksize is chosen as $K_F = 4$ in this case. It can be seen that the case with marginal pilot insertion in FD and TD shows the best performance. The case with equidistant pilot insertion in FD and TD performs worst although the distance between neighbouring pilots is smaller than for the marginal insertion. This effect is observable even for larger blocksizes if the marginal pilot insertion fulfils the sampling theorem in FD. For higher velocities, the performance gain of the marginal pilot insertion even increases.

In Figure 4(c), the DDCE is compared to the Wiener interpolation filter for the estimation of CVTD. It can be seen that for subcarrierwise pilot insertion with repetition, the DDCE clearly outperforms the Wiener interpolation filter. Due to the joint iterative filtering of the decision directed estimates, estimation errors caused by the estimation of CVFD can be mitigated by the application of DDCE. For the case that Wiener interpolation is applied for the estimation of CVFD, the Wiener interpolation for the estimation of CVTD slightly outperforms the DDCE. It can be stated, that DDCE is advantageous in cases of poor estimation performance for CVFD as it mitigates errors. Further investigations, which are not shown in this paper due to space limitations, have shown, that the reduction of the number Q_P of pilot symbols in FD leads to tremendous performance gains of DDCE compared to Wiener filtering.

6. CONCLUSION

It has been shown for B-IFDMA that chipwise pilot insertion provides lower PAPR than subcarrierwise pilot insertion for blocksizes $K_F > 2$, but exhibits a clearly worse estimation performance in combination with the applied estimation algorithm. For subcarrierwise pilot insertion with Wiener interpolation filtering for the estimation of CVFD and CVTD, the best estimation performance is achieved if the pilots are placed at the margins of the blocks of subcarriers in FD and at the margins of the TDMA slot in TD. Further, it has been shown, that DDCE improves the estimation performance tremendously compared to Wiener interpolation for the estimation of CVTD if the estimation performance for the estimation of CVFD is degraded.

REFERENCES

1. WINNERII. The WINNER II air interface: refined multiple access concepts. *Technical Report D4.6.1*, IST-4-027756 November 2006, viewed 09022010, wwwist-winnerorg/deliverables/D461pdf
2. Sorger U, De Broeck I, Schnell M. IFDMA—a new spread-spectrum multiple-access scheme. *Proceedings of ICC*, Atlanta, USA, 1998; 1013–1017.
3. Svensson T, Frank T, Eriksson T, Aronsson D, Sternad M, Klein A. Block interleaved frequency division multiple access for power efficiency, robustness, flexibility and scalability. *EURASIP JWCN* 2010; **2009**, Article ID 720973.
4. Ran J, Gruenheid R, Rohling H, Bolinth E, Kern R. Decision-directed channel estimation method for OFDM systems with high velocities. *Proceedings of 57th IEEE VTC*, Jeju, Korea, 2003; 2358–2361.

DOI: 10.1002/ett

5. Lam CT, Falconer D, Danilo-Lemoine F. Iterative frequency domain channel estimation for DFT-precoded OFDM systems using in-band pilots. *IEEE Journal on Selected Areas in Communications* 2008; **26**(2):348–358.
6. Sohl A, Klein A. Block-IFDMA – iterative channel estimation *versus* estimation with interpolation filters. *Proceedings of MC-SS*, Herrsching, Germany, 2009; 123–132.
7. Frank T, Klein A, Costa E, Schulz E. Low complexity equalization with and without decision feedback and its application to IFDMA. *Proceedings of PIMRC*, Berlin, Germany, 2005; 1219–1223.
8. Kay S. *Fundamentals of Statistical Signal Processing: Estimation Theory*. Prentice Hall PTR: New Jersey, USA, 1993.
9. Hayes MH. *Statistical Digital Signal Processing and Modeling* (1st edn). John Wiley & Son, Inc.: New York, USA, 1996.
10. Hoeher P, Kaiser S, Robertson P. Two-dimensional pilot-symbol aided channel estimation by wiener filtering. *Proceedings of ICASSP*, Munich, Germany, 1997; 1845–1848.
11. Robertson P, Villebrun E, Hoeher P. A comparison of optimal and sub-optimal map decoding algorithms operating in the log domain. *Procedings of ICC*, Vol. 2, Seattle, U.S.A., 1995; 1009 –1013.
12. Sari H, Karam G, Jeanclaud I. Frequency-domain equalization of mobile radio and terrestrial broadcast channels. *Proceedings of GLOBECOM*, San Francisco, U.S.A., 1994; 1–5.
13. Paetzold M. *Mobile Fading Channels* (1 edn). John Wiley & Sons Ltd.: Chichester, England, 2002.
14. Benvenuto N, Cherubini G. *Algorithms for Communications Systems and their Applications*. John Wiley & Sons Ltd.: Chichester, England, 2002.
15. van Nee R, Prasad R. *OFDM for Wireless Multimedia Communications* (1st edn). Artech House: Boston, MA, USA, 2000.
16. Sohl A, Frank T, Klein A. Channel estimation for DFT precoded OFDMA with blockwise and interleaved subcarrier allocation. *Proceedings of International OFDM Workshop*, Hamburg, Germany, 2006.

DOI: 10.1002/ett